Microchemical Journal 127 (2016) 36–45

Contents lists available at ScienceDirect

Microchemical Journal

journal homepage: www.elsevier.com/locate/microc

Vibrational spectroscopic study on degradation of alizarin carmine☆

Lea Legan [a,*], Klara Retko [a,b], Polonca Ropret [a,c]

[a] Research Institute, Conservation Centre, Institute for the Protection of Cultural Heritage of Slovenia, Poljanska 40, 1000 Ljubljana, Slovenia
[b] Faculty of Chemistry and Chemical Technology, University of Ljubljana, Večna pot 113, SI-1000 Ljubljana, Slovenia
[c] Museum Conservation Institute, Smithsonian Institution, 4210 Silver Hill Rd., Suitland, MD 20746, USA

ARTICLE INFO

Article history:
Received 11 January 2016
Accepted 3 February 2016
Available online 11 February 2016

Keywords:
Alizarin carmine
Alizarin red S
Degradation
Reflection FTIR
SERS
Artworks

ABSTRACT

Identification of organic dyes together with possible degradation products is often complicated in the field of cultural heritage. The main focus of this work is utilization and comparison between non-invasive reflection infrared spectroscopy, transmission infrared spectroscopy, and surface-enhanced Raman spectroscopy (SERS), a minimally invasive technique in order to understand the ageing behaviour of paint layers containing organic dye alizarin carmine (alizarin red S, sodium alizarin sulfonate, ARS) in lipid and proteinaceous binder. The results obtained with both Fourier transform infrared (FTIR) spectroscopies highlight a significant degradation of ARS paint layers where changes in hydroxyl, sulfonate, and carbonyl groups of alizarin red S were observed. In most of the cases, the intensity of IR bands belonging to the degraded alizarin red S was so weak or shifted that would make its positive identification questionable in an unknown sample. After all, it was apparent that SERS is a powerful technique to detect even the trace ARS molecules. Furthermore, degradation was even more pronounced for the paint layers of ARS combined with linseed oil. Namely, a transparent white layer of sodium sulfate was formed above the aged ARS glaze layer.

1. Introduction

Organic colorants have been an important part of artist's pallet since ancient times. They could be extracted from natural sources such as plants (e.g., madder roots) or animals (e.g., cochineal) [1,2]. Anthraquinones have been frequently used as important coloring materials for different artistic objects, such as archaeological textiles [3,4], manuscripts, drawings, or paintings [5]. For glaze layers, they were used for giving depth, to enrich shadows, or to make dull colors more vivid. After the synthesis of 1,2-dihydroxyanthraquinone (alizarin), synthetic materials in many aspects substituted the natural ones. Alizarin carmine (1,2-dihydroxyanthraqinone-3-sulfonate; alizarin red S, ARS) (see Fig. 1) was discovered in 1871 by Graebe and Libermann as a water-soluble version of naturally occurring reddish dye alizarin [6]. ARS as a water-soluble dye can exist in aqueous solutions in three different forms: in neutral form, anionic, and dianionic form [7]. Hydroxyanthraquinones have a very wide range of applications. Beside dye industry, they are also used in histochemistry [8], medicine, food industry [9], etc. Alizarin red S shows a potential to be used as an organic analytical reagent for the determination of inorganic substances (such as Ca, Al) [10,11], biological active compounds, photosentisizer [12], and selective depressant in the separation of minerals [7,13]. Samples of cultural heritage show great heterogeneity and several different microscopic, spectroscopic, chromatographic, etc., methods have been developed for their characterization, which is together with the detection of their degradation products very challenging. Regarding the priceless value of cultural heritage objects and therefore limited sampling, there is a demanding task in conservation science in development of scientific methods that could be applied in minimally invasive and destructive manner with no or minimal interventions to keep the integrity of a work of art. Vibrational spectroscopy is frequently used for the spectral characterization of artist materials [14,15] as well as for monitoring of degradation processes of different organic colorants [16–18]. It was found that organic pigments, namely, alizarin, permanent red, and phthalocyanine green mixed with linseed oil, degraded under the UV light exposure, specifically breaking both aromatic rings in the organic pigments' and binder's unsaturated fatty acid C = C bonds [16]. The assessment of ageing processes occurring in natural dyes (indigo, madder, curcumin, carmine acid, and dragon's blood) used in oil and watercolor paintings was made by Koperska et al. [17]. It was shown that the degradation of dyes is dependent on the molecule symmetry. The more is a molecule symmetrical, the less is prone to degradation [17]. Irreversible photoassisted degradation of dye, alizarin red S, under UV light radiation and the presence of photocatalytic TiO_2 were examined by Liu et al. [18]. Degradation products, such as phthalic acid and other carbonyl species, suggest the decay of C-C bond near the C = O group of ARS molecule (see Fig. 1), while remaining multihydroxylated species decompose further to smaller fragments (e.g., CO_2 and SO_4^{2-} ions) [18]. Furthermore, utilizing a conventional transmission FTIR

☆ Selected papers presented at TECHNART 2015 Conference, Catania (Italy), April 27–30, 2015.

* Corresponding author.
E-mail addresses: lea.legan@zvkds.si (L. Legan), klara.retko@zvkds.si (K. Retko), polona.ropret@zvkds.si (P. Ropret).

http://dx.doi.org/10.1016/j.microc.2016.02.002
0026-265X/

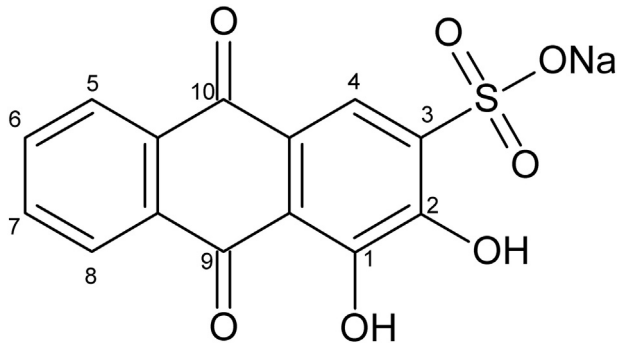

Fig. 1. Chemical structure of alizarin red S molecule.

analysis numerous studies have been performed concerning the molecular information of organic dyes [14,19–21], but the method demands sampling, which can result in the loss of information from the surface. Non-invasive reflection FTIR measurements provide valuable information about the molecular composition as well as degradation processes of artworks' surfaces, although the interpretation of spectra is often very challenging [22–24]. To our knowledge, the non-invasive reflection FTIR spectroscopy has not been used for degradation studies of organic glaze layers. On the other hand, the problem with using FTIR spectroscopy for analysis of paint layers consisting of organic colorants derives from the interfering signal of the binders and/or other inorganic components, which could be present in other layers (for example, calcium carbonate in the ground layer). In such cases, surface-enhanced Raman spectroscopy (SERS) can be utilized in order to gain more information on the classification of the organic dyestuffs. It has already proved to be effective in the investigations in the field of cultural heritage [25–27] and in characterization of anthraquinones and its derivatives [28–35]. SERS is a sensitive analytical technique as the signal of compounds with weak Raman scattering properties in the vicinity of certain nanostructures is enhanced in addition to reduction of fluorescence effects [36]. Several authors also report on single-molecule detection [37,38].

This work focuses on the application of non-invasive reflection Fourier transform infrared (FTIR) spectroscopy, transmission FTIR spectroscopy, and minimally invasive surface-enhanced Raman spectroscopy (SERS) for assessing degradation processes of paint layers of alizarin carmine bound in two binders with different chemical composition (linseed oil and egg tempera). In order to better understand the reflection spectral anomalies of aged ARS paint layers, several techniques such as conventional Raman, infrared spectroscopy, and electron microscopy with energy dispersive spectroscopy (SEM /EDS) were complemented.

2. Experimental

2.1. Materials

Animal glue (No. 63028), chalk from Bologna, light (No. 58150), pigment cinnabar (HgS; No. 42000) and organic dye alizarin carmine (alizarin red s, sodium salt of 1,2-dihydroxyanthraquinone-3-sulfonate, ARS; No. 94,150) were supplied by Kremer Pigmente GmbH & Co. KG. Sun-bleached linseed oil was purchased from Lefrance & Bourgeois. Eggs were bought from the local market. Other chemicals, which served in preparation of HPC-based photoreduced silver colloid for SERS analysis, namely, silver nitrate ($AgNO_3$; No. 209139) and hydroxypropyl cellulose (HPC; No. 191906) were provided by Sigma-Aldrich.

2.2. Preparation of model painting and artificial ageing

Two model paintings were prepared according to art technology [39,40] in order to imitate the structure of a canvas painting. Linen canvas was attached to a wooden stretcher, sized with animal glue solution, and impregnated with gesso ground. Pigment cinnabar was ground with linseed oil and non-fatty egg tempera with pigment to binder weight ratio of about 5:1 and 2:1, respectively, and applied on top of the ground layer. After drying, a thin layer of colorant alizarin carmine, mixed with the same binders as the cinnabar containing layer, was applied on top. Colorant alizarin carmine was mixed with linseed oil in weight ratio of about 1:6 and with egg yolk binder in weight ratio 1:4. One of the model paintings was then exposed to accelerated artificial ageing in climatic chambers with well-defined and controlled temperature, relative humidity, and light conditions. A metal halide lamp (2000 W, OSRAM HQI-TS 2000 WDS; Osram GmbH, Germany), equipped with window glass filters, was used for the simulation of light radiation, which was a good simulation of daylight filtered through glass. Light intensity was near zero in the λ range of 300–400 nm and approximately 800 Wm^{-2} in the λ range of 400–800 nm.

Model painting was exposed to a metal halide lamp for a period of 30 days and followed by exposure in a climatic chamber with oscillations of temperature and relative humidity for another 30 days. One ageing cycle in the climatic chamber lasted 210 min wherein the temperature varied between 5 °C and 40 °C with an average velocity 0.56 °C/min and relative humidity varied from 20% to 90%.

2.3. Instrumentations

2.3.1. FTIR investigations

2.3.1.1. Transmission mode. FTIR transmission spectra were recorded using a Perkin Elmer Spectrum 100 FTIR spectrophotometer coupled to a Spotlight FTIR microscope equipped with nitrogen cooled mercury-cadmium telluride (MCT) detector. The samples taken from the model painting were placed between the windows of a diamond anvil cell and examined under microscope with aperture of 50 × 50 μm. The spectra were collected in the range between 4000 and 600 cm^{-1}, at 4 cm^{-1} spectral resolution and with an average of 64 spectral scans accumulated. Additionally, the transmission FTIR spectra of pure colorant ARS were collected using a KBr pellet method in the range of 4000–450 cm^{-1}.

2.3.1.2. Reflection mode. Reflection FTIR analyses were carried out with a portable Bruker ALPHA-R spectrometer, equipped with a dedicated reflection module, which allows contactless and non-destructive FTIR analysis with a room temperature DLaTGS detector. The samples were placed in front of the instrument at a distance of about 1 cm, and the integrated video camera provided the view of the sampling area of about 28 mm^2. Reflection spectra were collected in situ in the range of 5500–600 cm^{-1}, at the spectral resolution 4 cm^{-1} over 160 scans. The background was acquired using a gold mirror as a reference sample. The Kramers–Kronig algorithm was not applied in obtained total reflection spectra due to contribution of specular and/or diffuse components of reflected light, which can result in irregularities in the corrected spectra. [22–24].

With transmission and reflection mode, three different spectra were obtained for each sample. All the spectra were then baseline corrected and averaged using the OPUS 7.0 data collection software package (Bruker, Germany). FTIR spectra are presented in absorbance and pseudo-absorbance units.

2.3.2. Raman and SERS investigations

The spectra of the samples were recorded using a 785 nm and 514 nm laser excitation lines with a Horiba Jobin Yvon LabRAM HR800 Raman spectrometer coupled to an Olympus BXFM optical microscope. The spectra were recorded using ×100 objective lens and/or ×50 long working distance objective lens, and a 600 grooves/mm grating. A multi-channel, air-cooled CCD detector was used, and the spectral range was set between 300 and 1800 cm^{-1} for obtaining spectra with $\lambda_0 = 514$ nm (SERS and conventional Raman) and between 400 and 1800 cm^{-1} for conventional Raman measurement using $\lambda_0 = 785$ nm.

The wave number calibration was performed using a silicon wafer. For the SERS analysis, a drop of a SERS substrate was deposited on a small amount of powder samples (pure dye ARS) or on the surface of the minute samples, taken from the model panels. All the SERS spectra were averaged (15 spectra) using the OPUS 7.0 data collection software package (Bruker, Germany). The SERS substrate (silver nanoparticles are spherical, not homogeneous in size, but have a most populate size range of 20–60 nm diameter) used in this study was the HPC-based photoreduced substrate. The characterization and the use of this substrate to study cultural heritage samples was already presented in one of our previous work [41]. Briefly, silver nitrate and HPC (hydroxypropyl cellulose) were dissolved in miliQ water to achieve a weight ratio between $AgNO_3$ and HPC of 1:0.6. The solution was stirred for 2 days at room temperature so that the HPC was completely dissolved and swelled. The substrate was then exposed to ultraviolet irradiation, which induced and/or accelerated the reduction of silver ions to silver nanoparticles, which served for Raman signal enhancement of fluorescent dye alizarin carmine.

2.3.3. Electron microscopy with energy dispersive spectroscopy (SEM/EDS)

Polished cross sections were investigated using scanning electron microscope (SEM) JEOL 5500 LV, Japan, in a rough vacuum (12 Pa), wherein cross-sectional areas of the samples were not necessary to be additionally coated with graphite or gold layer. The accelerating voltage of 20 kV was applied. Energy dispersive spectroscopy (EDS), Oxford Instruments INCA, Great Britain, was used for image capture and for qualitative and quantitative elemental analysis of selected areas.

3. Results and discussion

Alizarin carmine (alizarin red S, ARS) is a synthetic derivative of 1,2-dihydroxyanthraquinone known as alizarin. Its chemical structure is presented in Fig. 1. In comparison to alizarin, it has an additional sulfonate group, which is bound to the anthracene ring (carbon at the site 3). A systematic approach in the investigation of ARS paint layers was conducted in order to understand chemical behaviour of paint layers affected by artificial ageing. Pure colorant powder was examined by different spectroscopic methods (namely, invasive and non-invasive FTIR spectroscopy, Raman, and SERS spectroscopy). Results of degradation of ARS paint layers, which were applied atop cinnabar paint layers, are discussed in the following sections for each binder separately. Cinnabar was selected for the preparation of the layer beneath the glaze in order to replicate artists' glaze layers structure and as it does not have any absorption in the mid IR spectral range; therefore, it does not affect the investigation of ARS glaze layers. The numerical frequencies observed with non-invasive reflection and conventional transmission FTIR spectroscopy are summarized in Tables 2 and 3, together with tentative assignments for alizarin carmine [28,29,42–45] and specific binders [46,47].

3.1. Infrared, normal Raman, and SERS spectra of pure alizarin carmine

There are numerous reports on the identification and characterization of alizarin carmine (ARS) by traditional FTIR spectroscopy [28,29,42–45] and SERS using various types of substrates [31]. However, to validate the detection of the dye, and to set the baseline for the demonstration of the non-invasive procedure (reflection FTIR, Section 3.2), as well as to show superior performance of ARS by AgHPC substrate, spectra of the pure colorant powder were recorded in ideal conditions by transmission FTIR, Raman, and SERS methods and are summarily presented in Fig. 2. ARS is fluorescent and does not produce sufficient Raman signal at the presented conditions. In addition, the luminescence obscures the spectrum resulting in high background (see Fig. 2b, gray line). Therefore, SERS can offer a solution for its detection as the Raman signal is amplified above the fluorescence signal. ARS can interact (similar as alizarin) with the nanoparticle surface through hydroxyl and keto

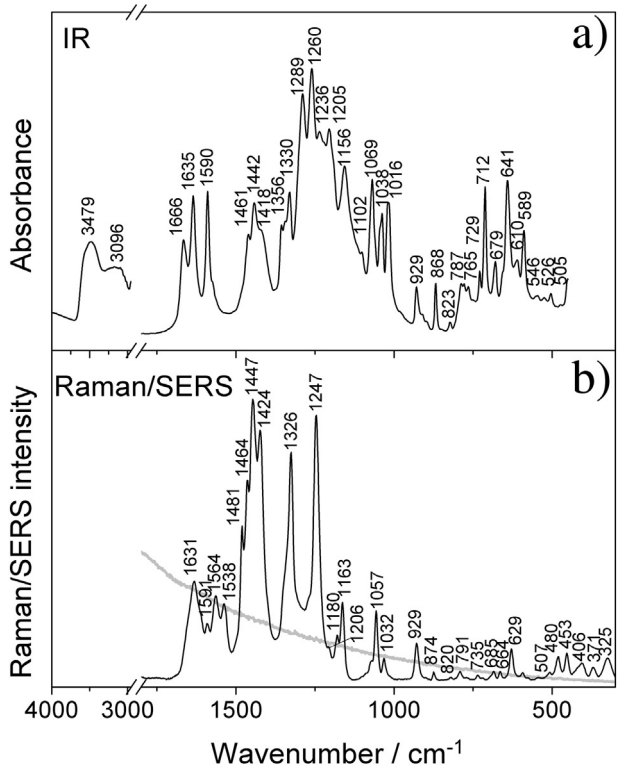

Fig. 2. (a) Absorption FTIR spectrum of pure ARS in KBr; (b) Normal Raman (gray line) (λ_0 = 514 nm, 0.01 mW, 2 s exposure time) and SERS (black line) spectra of ARS powder (λ_0 = 514 nm, 0.6 mW, 5 s exposure time).

groups. Corresponding SERS spectra are pH-, excitation wavelength-, and concentration-dependent [28]. In this study, SERS offered both Raman signal enhancement in addition to fluorescence quenching (see Fig. 2b, black line). The transmission FTIR spectrum (using the standard KBr pellet method) of ARS is shown in Fig. 2a. Band wave numbers of pure ARS powder and their tentative assignments are reported in Table 1.

Briefly, in SERS, and IR spectra, the main common features were observed:

- Stretching vibrations of carbonyl group between 1630 and 1670 cm^{-1}
- Aromatic CC stretching vibrations at ~1590 cm^{-1}
- Several bands between 1420 and 1500 cm^{-1}, which can be assigned to combinations of vibrations of ether CC, COH, CO, or CH groups
- Stretching vibration of CC group at ~1330 cm^{-1}
- Strong IR signal at ~1205 cm^{-1} and a weak SERS band at ~1206 cm^{-1}, which can be assigned as stretching and bending modes of three carbons (i.e., the middle carbon belongs to 9- or 10-C = O carbon (see Fig. 1), and the other two carbons belong to both sides of the middle carbon) in the anthracene skeleton
- Medium strong bands at ~1069 and ~1156 cm^{-1} correlate to symmetric and asymmetric stretching of sulfonate group

3.2. Paint layers of alizarin carmine in linseed oil

3.2.1. Non-invasive reflection FTIR spectroscopy

Non-invasive reflection FTIR spectra of aged and unaged ARS paint layers in linseed oil are gathered in Fig. 3. In the total reflection spectrum obtained on the unaged ARS paint layers, the characteristic bands of ARS colorant and linseed oil binder (see Fig. 3_black line and Table 2) could be observed, while in the spectrum of the artificially aged ARS paint layers, most of the vibrational frequencies of ARS

Table 1
Numerical frequencies observed in IR and SERS spectra of the pure ARS powder with tentative assignments.

IR[a] (cm^{-1})	SERS[a] (cm^{-1})	Band assignment[b] Alizarin red S [28,29,31,42–45],
	325 vw	skeletal vibrations
	371 vw	
	406 vw	
	453 vw	
	480 vw	
505 vw	507 vw	
526 vw		
546 vw		
589 m		
610 w		
641 m	629 vw	
679 w	664 vw	γ (C = O)/δ (CCC)
712 m	685vw	γ (C = O)/γ (C-O)
729 vw	735 vw	δ (CCC)
765 w		γ (C-H)/γ (C = O)/τ (CCCC)
787 w	791 vw	
823 vw	820 vw	γ (C-H)/γ (C-O)
868 w	874 vw	
929 w	929 w	
1016 m		ν (CC)/δ (CCC)
1038 m	1032 w	δ (CCC) //ν(CC)/δ (CH)
1069 m	1057 m	υ_S (SO_3)
1102 w		
1156 m	1163 m	υ_{AS} (SO_3)
	1180 w	ν (CC)/δ (CH)/δ (CCC)
1205 s	1206 sh	ν (C = O)/δ (CCC)
1236 s		hydrous SO_3
	1247 vs	ν (C = O)
1260 vs		υ (1-C-O)
1289 vs		υ (2-C-O)
1330 m	1326 vs	ν (CC)
1356 m		ν (C-C)/δ (COH)
1418 m	1424 vs	
1442 m	1447 vs	ν (CC) arom.
1461 m	1464 s	ν (CC)/δ (COH)/δ (CH)
	1481s	ν (C = O)/ν (CC)/δ (CH)
	1538 m	ν (CC) arom.
	1564 m	ν (CC) arom.
1590 m	1591 w	ν (CC) arom.
1635 m	1631 m	ν (9-C = O)
1666 m		ν (10-C = O)
3096 sh		intramolecular hydrogen bonding ν (OH)
3479 m, br		ν (OH)

[a] vw—very weak, w—weak, m—medium, s—strong, vs—very strong, sh—shoulder.
[b] ν—stretching, δ—in-plane bending, γ—out-of-plane bending, τ—torsion.

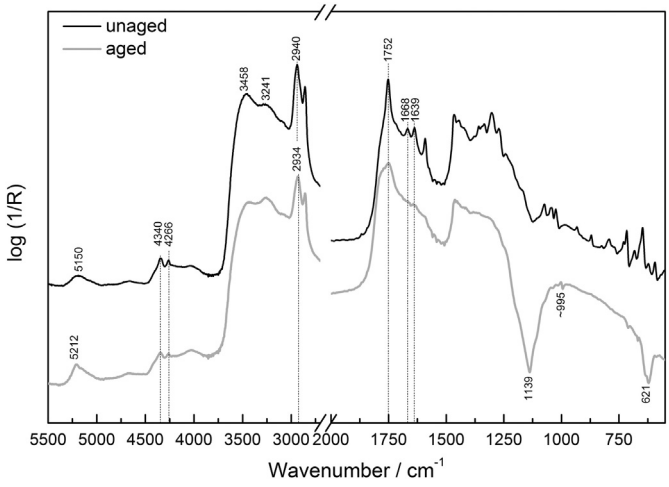

Fig. 3. Non-invasive reflection FTIR spectra of unaged (black spectrum) and aged (gray spectrum) ARS linseed oil paint layers. Spectra are translated upon vertical axis for ease of comparison. The most representative differences between spectra are labelled.

colorant are no longer visible (see Fig. 3_gray line and Table 2). One of the two characteristic absorption bands, namely, ν(10-C = O) frequency, in the spectrum obtained after ageing disappears, while the second one (ν(9-C = O)) is observed as a shoulder at 1639 cm^{-1} on the strong and broaden band of carbonyl-stretching mode of lipid medium. The ageing process affects the other moieties of ARS molecule. For instance, all the aromatic skeletal modes and residual vibrations of anthracene ring are no longer visible after ageing. Changes in band shape are observed also in the OH stretching region. Strong band of ν(OH) of ARS molecule decreased during ageing, while the band of ν(OH), related to lipid binder, increased in relative intensity, suggesting a strong degradation of ARS paint layer as well as lipid binder. Furthermore, few changes appeared also in the shape and position for other distinctive bands of lipid binder. Indeed, the strong stretching vibration mode of carbonyl group, observed at 1752 cm^{-1}, is broadened in the spectrum of the aged layer, as well as the asymmetric stretching vibration of CH group is shifted by 6 cm^{-1}. Downshift and broadening is observed in the signal of asymmetric bending vibration of linseed oil methyl group (see Table 2). All these results obtained after artificial ageing indicating a progressive oxidation on the alkylic chains of linseed oil [48,49].

Further information on the layers behaviour beneath the surface was possible to obtain from the spectra in the near infrared range. The lipid binder in the near-IR range of reflection spectrum shows characteristic signals of combination bands of methylenic C-H stretching and bending vibrations at 4340 and at 4266 cm^{-1} [50,51]. Those bands are weakened in the spectrum of the aged paint layer. Furthermore, the near-IR region of unaged model sample reveals another combination band of asymmetric stretching and bending vibration of hydroxyl group at 5150 cm^{-1}, which is characteristic for gypsum (ground layer). The band is shifted toward higher wave number after ageing and is visible as a single sharp band at 5212 cm^{-1}, which is typical for bassanite [52]. This observation indicates that during ageing, gypsum in the ground layer loses part of its bonded water, which leads to the transformation into the hemihydrate form.

Furthermore, in the total reflection spectrum of aged ARS paint layers in linseed oil, additional spectral features were observed (see Table 2). An inverted (*reststrahlen*) band with minimum at 1139 cm^{-1} occurred due to high absorption index *k* of investigated material and belongs to SO_4^{2-} asymmetric stretching vibrations [22]. The same distortion effect goes for asymmetric bending vibration of sulfate group and is placed at 621 cm^{-1}. Symmetric stretching vibration of the same group is seen as derivative-like band in the range from 900 to 1000 cm^{-1}.

In order to verify the sulfate stretching and bending spectral features in the non-invasive reflection FTIR spectrum obtained on the aged ARS paint layers, additional analyses were performed. Electron microscopy with energy dispersive spectroscopy (SEM/EDS) was used to study the chemical composition of the transparent white layer, which was newly formed atop of lipid ARS glaze layer after accelerated ageing. Results obtained on the two points (marked in Fig. 4 as 1a and 2a) of the uppermost layer on the polished cross section revealed the occurrence of grains made of sodium, sulfur, and oxygen that can be attributed to sodium sulfate (Na_2SO_4) (see Fig. 4a,b). Most likely, the oxidation of sulfonate group lead to formation of sodium sulfate.

In agreement with SEM/EDS results, the formation of sodium sulfate was confirmed also with conventional Raman spectroscopy. The Raman spectrum (Fig. 4c) was obtained on the same point of the uppermost layer of the polished cross section (Fig. 4a) as for SEM/EDS analysis (Fig. 4b) in the range between 1800 and 400 cm^{-1}. The main band placed at 996 cm^{-1} corresponds to sulfate symmetric stretching vibrations. A weak asymmetric stretching triplet of sulfate anion occurs between 1100 and 1160 cm^{-1}. The asymmetric bending vibration of SO_4^{2-} is visible as very weak triplet at 646, 636, and 621 cm^{-1}. Another broadened and weak band, which correlates to symmetric bending vibration of sulfate anion has its maximum at 460 cm^{-1} [53].

Table 2
Numerical frequencies observed in reflection and transmission FTIR spectra of the ARS paint layers in linseed oil before and after artificial ageing.

Transmission FTIR[a] (cm^{-1})		Reflection FTIR[a] (cm^{-1})		Band assignment[b]	
Before ageing	After ageing	Before ageing	After ageing	Alizarin red S [28,29,42,43,44,45]	Linseed oil [46,47]
		592 w		skeletal vibrations	
617 w	614 w	620 w			
			$621_{\text{reststrahlen band}}$	$\nu_4\ (SO_4^{2-})$	
640 m	640 w	644 m		skeletal vibrations	
680 w	679 m	680 w		γ (C = O)/δ (CCC)	
712 m	714 w	713 m		γ (C = O)/γ (C-O)	
729 vw	728 vw	729 vw		δ (CCC)	
767 w	766 sh	764 vw		γ (C-H)/γ (C = O)/τ (CCCC)	
780 w	779 vw				
788 w		788 w			
823 vw	823 vw	825 vw		γ (C-H)/γ (C-O)	
870 w	870 vw	869 w			
930 w	930 w	929 w			
			990–1000	$\nu_1\ (SO_4^{2-})$	
1021 m	1020 m	1018 m		ν (CC)/δ (CCC)	
1039 m	1044 m	1040 m		δ (CCC) //ν(CC)/δ (CH)	
1071 m	1070 sh	1070 m		$\upsilon_S\ (SO_3)$	
	1130 sh		$1139_{\text{reststrahlen band}}$	$\nu_3\ (SO_4^{2-})$	
1159 vs	1160 vs	1158 sh		$\upsilon_{AS}\ (SO_3)$	
1203 vs				ν (C = O)/δ (CCC)	
1235 s		1230–1240		hydrous SO_3	
1260 vs	1255 sh	1250–1276		υ (1-C-O)	
1289 s	1286 s	1280–1300		υ (2-C-O)	
1330 m	1330 m	1333 s		ν (CC)	
1344 m, sh	1344 m, sh				
1357 m		1360 s		ν (C-C)/δ (COH)	
			1383 w		$\delta(CH_3)$ umbrella mode
1418 m	1418 sh				
1442 m	1443 m	1445 s	1453 s	ν (CC) arom.	
1461 m	1460 sh	1465 s	1462 s	ν (CC)/δ (COH)/δ (CH)	$\delta_{AS}\ (CH_3)$
1591 m	1591 m	1592 s		ν (CC) arom.	
1636 m	1638 m	1639 s	1639 sh	ν (9-C = O)	
1666 m	1668 m	1668 s		ν (10-C = O)	
1740 s	1740 s	1752 vs	1752 vs, br		ν (C = O)
2857 m	2858 m	2860 vs	2860 vs		$\nu_S\ (CH_2)$
2931 s	2931 m	2940 vs	2934 vs		$\nu_{AS}\ (CH_2)$
3074 sh	3075 sh	3098 vw	3097 vw	intramolecular hydrogen bonding ν (OH)	
3240 m, br	3240 w, br	3241 br	3264 s	ν (OH)	ν (OH)
3460 m, br	3460 w, br	3458 s	3435 br	ν (OH)	

[a] vw—very weak, w—weak, m—medium, s—strong, vs—very strong, sh—shoulder, br—broad.
[b] ν—stretching, δ—in-plane bending, γ—out-of-plane bending, τ—torsion.

3.2.2. Transmission FTIR spectroscopy

Fig. 5 reports the transmission FTIR spectra of aged and unaged paint layers of ARS in linseed oil. The spectrum of non-aged ARS paint layer in linseed oil (Fig. 5_black line) exhibits all characteristic vibrational bands of ARS colorant and is in agreement with results for pure ARS powder presented in Fig. 2a. In contrast to non-invasive FTIR spectrum, the transmission spectrum of the aged ARS paint layer indicate less extensive changes of the bands characteristic for the organic dye. This might arise due to a higher concentration of the unchanged ARS in the bulk comparing to the surface. Further differences can be a consequence of a possible change of paint morphology at the surface due to ageing to which reflection FTIR might be more sensitive. The most observable change in the spectrum of the aged ARS paint layer acquired by transmission (see Fig. 5_gray line) is seen in the absence of two strong bands dedicated to stretching vibrations of hydrous sulfonate group and to combination of stretching and bending modes of three carbons in the anthracene skeleton (bands at 1235 and 1203 cm^{-1}). Furthermore, the symmetric stretching vibration of sulfonate group decreased in intensity during ageing and is visible as a shoulder of the stronger ν_{AS} (SO_3) at 1160 cm^{-1}. Another shoulder band, placed at 1130 cm^{-1}, occurs as a new formed band after ageing, and it can be attributed to asymmetric stretching vibrations of sulfate group related to the transparent white layer of sodium sulfate. These results suggest that the sulfonate group is strongly affected by the ageing process. The oxidation of sulfonate group leading to formation of sodium sulfate was therefore confirmed also by transmission IR approach.

The very strong signal of stretching vibration of 1-CO group at 1260 cm^{-1} is in the spectrum obtained after ageing shifted to lower wave numbers by ~5 cm^{-1} and is apparent as a shoulder band of the stronger asymmetric stretching mode of sulfonate group.

Additional changes in band shape and position are visible in the combination band of CC stretching and COH bending vibration. More precisely, after the ageing, signal at 1357 cm^{-1} is no longer visible, whereas the shoulder band at 1344 cm^{-1} increases in intensity. Two medium strong bands placed at 1461 and 1418 cm^{-1} decreased in intensity and are visible as shoulder bands of the stronger aromatic CC stretching vibration at 1443 cm^{-1} in the spectrum obtained on the aged ARS paint layer. Loss of intensity is detected also in combination band of γ (C = O)/γ(C = O)/τ (CCCC) vibrations after ageing. Two signals placed at 712 (γ(C = O)/γ (C-O) and 680 cm^{-1} (γ(C = O)/δ (CCC)) show variations in the relative intensity after ageing. The first one is weakened and the latter one increased in intensity.

The reduction in relative intensity is also visible in both broadened bands of hydroxyl stretching vibrations of ARS colorant as well as of linseed oil medium placed at 3460 and 3240 cm^{-1}, respectively. Moreover, all distinctive spectral features of linseed oil are considerably diminished (see Fig. 5 and Table 2) after ageing. These findings concerning lipid binder indicate an occurring oxidative degradation [48]. Photo-oxidation of linseed oil takes place in several stages and it

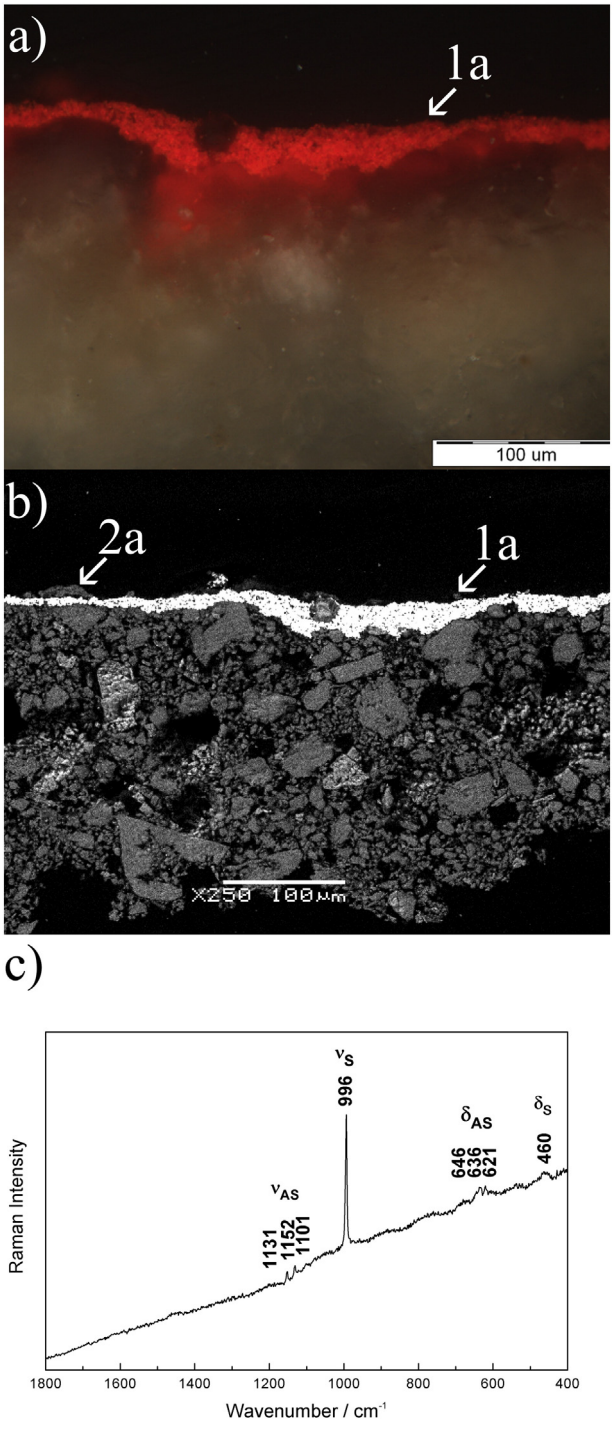

Fig. 4. (a) Optical and (b) SEM image of the sample taken from the aged model painting with marked locations of EDS analysis, identifying Na_2SO_4. (c) Raman spectrum of sodium sulfate obtained at the surface of aged paint layers of ARS in linseed oil (location of Raman analysis is marked as 1a) ($\lambda_0 = 785$ nm, 3 mW, 5 s exposure time).

appears as continuation of progressive hardening process [48,54]. During oxidation processes, many different radical species are formed, such as alkoxyl, alkyl, peroxy, and hydroxyl radical, etc., which can during the hardening process recombine and form tridimensional network [55]. Photo-oxidation causes partial fragmentation of tridimensional network and evolution of free radicals, low molecular weight compounds, alkylic fragments, etc. The layer of sodium sulfate above the paint layers of ARS in linseed oil could be explained by the formation of hydroxyl radical during the binder's photo-oxidative degradation.

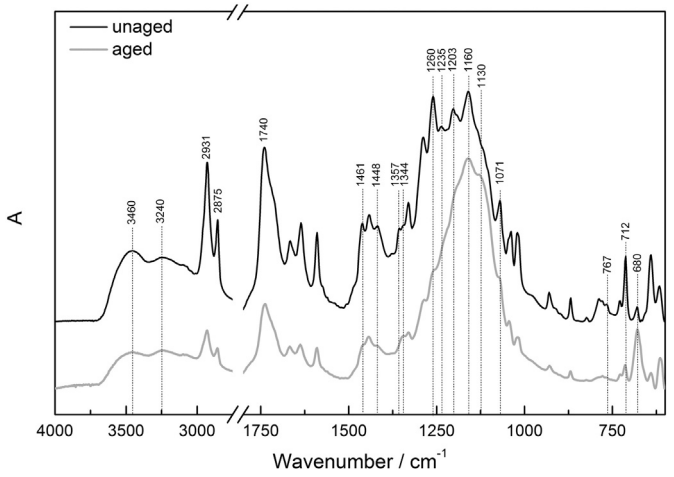

Fig. 5. Transmission FTIR spectra of unaged (black spectrum) and aged (gray spectrum) ARS linseed oil paint layers. Spectra are translated upon vertical axis for ease of comparison. The most representative differences between spectra are labelled.

Attack of hydroxyl free radical on the sulfonate moiety of ARS molecule can lead to the formation of sulfate ions [56]. An assumed degradation mechanism is given in Scheme 1.

3.2.3. Surface-enhanced Raman spectroscopy (SERS)

SERS spectra of the organic dye bound in linseed oil (aged and unaged paint layers) are presented in Fig. 6. The main differences between the spectra of unaged and aged paint layers are the variations in relative intensities of the bands between 1400 and 1450 cm^{-1} and 1540–1650 cm^{-1}. SERS spectrum of powder ARS has in the region between 1400 and 1450 cm^{-1} two characteristic bands (at 1424 and 1447 cm^{-1}, the latter having higher intensity). In the unaged paint layer, also the band at ~1442 cm^{-1} shows a high intensity, while the band at 1428 cm^{-1} appears as a shoulder. In the aged color layers, there is reversed band intensity—the band with higher intensity being at 1428 cm^{-1}. Those bands are associated with the stretching modes of aromatic ring. Furthermore, after the artificial ageing, the weak band at 1176 cm^{-1} (ν (CC)/δ (CH)/δ (CCC) [28] appears as a shoulder in the spectrum of the aged layer, bands at 1565 and 1541 cm^{-1} disappear, and a new broad band emerges at 1549 cm^{-1}. The increase in the band at 1549 cm^{-1}, which involves either CC stretching [28] or carbonyl stretching [7], should appear as a consequence of a change in resonance structure. Moreover, the strongest band in the carbonyl-stretching region appears at 1634 cm^{-1} in the spectrum of unaged paint layer, while in the spectrum of aged paint layer at 1619 cm^{-1}. Similar results were obtained by Holmgren et al. [7], when the pH dependence of ARS in DRIFT spectra were studied and by Cañamares et al. [28], which explained the effect on SERS spectra regarding to different adsorption modes of alizarin on silver nanoparticles' surface. Because the changes in the SERS spectra of ARS are visible mainly in the region of vibrations associated with different adsorption modes of ARS on nanoparticle surface, we suggest that the variations are a consequence of different ARS interaction with silver nanoparticles' surface and/or the changes in the resonance structure [7,28,31]. For the aged paint layer, it could be proposed, especially based on the increase of the band at 1421 cm^{-1}

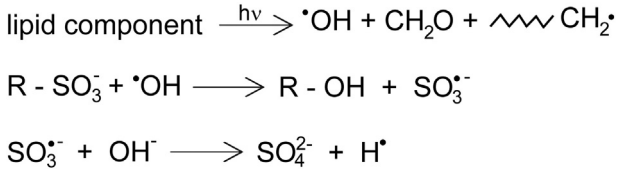

Scheme 1. Proposed degradation mechanism of ARS molecule in linseed oil paint layers.

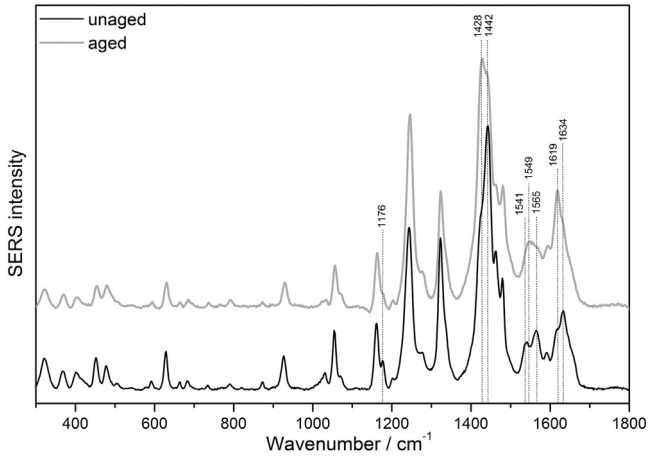

Fig. 6. SERS spectra of unaged (black spectrum) and aged (gray spectrum) ARS linseed oil paint layers. Spectra are translated upon vertical axis for ease of comparison. (λ_0 = 514 nm, 0.6 mW, 5 s exposure time).

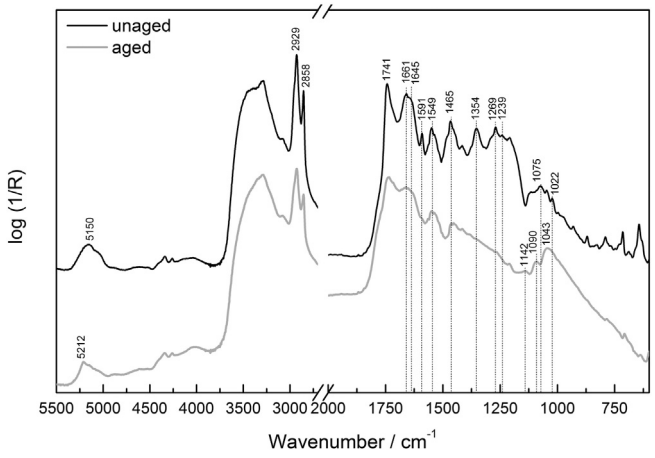

Fig. 7. Non-invasive reflection FTIR spectra of unaged (black spectrum) and aged (gray spectrum) ARS egg tempera paint layers. Spectra are translated upon vertical axis for ease of comparison. The most representative differences between spectra are labelled.

(which is also very intense in the spectrum of alizarin using the same substrate and associated to the dianionic form), that the adsorption mode of ARS in the aged samples is preferentially dianionic. ARS adsorbs strongly with the primary adsorption sites, which further leads to deprotonation of OH-group. Furthermore, this could be possibly also correlated to different concentration of ARS dye in the unaged and aged samples, suggesting a higher concentration of ARS in unaged paint layers. In such cases, when the concentration of analyte is low, ARS adsorbs strongly with the primary adsorption sites, which further leads to deprotonation of OH-group; therefore, a higher contribution of ARS in dianionic form is visible in the SERS spectrum of the aged paint layers.

Interestingly, no significant changes of the bands assigned to sulfonate group are visible as in the case of IR spectroscopy results. The explanation most likely reflects the fact, that ARS adsorbs through keto and hydroxyl sites, and the sulfonate groups is the most distant group from the nanoparticle surface and therefore the least affected by the influence of the nanoparticle and the SERS effect. Furthermore, the bands associated with sulfonate vibration modes could also be overlapped by the anthracene skeletal vibration modes.

3.3. Paint layers of alizarin carmine in non-fatty egg tempera

3.3.1. Non-invasive reflection FTIR spectroscopy

The non-invasive reflection FTIR spectra of artificially aged and unaged ARS paint layers in non-fatty egg tempera are presented in Fig. 7. The most pronounced changes in the medium IR range during ageing involve the absence of two strong bands placed at 1591 and 1354 cm^{-1} that are assigned to aromatic CC stretching vibration and combination of CC stretching and COH bending vibrations, respectively (see Table 3). Additionally, a decay of band intensity at 1661 cm^{-1} was observed, which corresponds to carbonyl-stretching vibration of ARS molecule. Another loss of intensity is seen in the signal of combination of ν (CC)/δ (COH)/δ (CH) vibrations placed at 1465 cm^{-1}. Similarly, as for the non-invasive reflection monitoring of degradation of ARS paint layers in lipid binder, the strong band of stretching vibrations of 1-CO group at 1269 cm^{-1} along with the stretching vibrations of hydrous sulfonate group at 1239 cm^{-1} are no longer visible in the spectrum obtained after ageing. Asymmetric stretching vibration of sulfonate group is seen as distorted derivative-like/inverted band in the range of 1135–1200 cm^{-1} in the reference spectrum, whereas the same signal is broadened and has its maximum at 1142 cm^{-1} in the spectrum of the aged paint. In parallel, the symmetric band of aforementioned group at 1075 cm^{-1} is shifted by 20 cm^{-1} to higher wave numbers. The changes in the sulfonate regions are visible to a lesser extent as in the case of ARS in linseed oil paints. Also, no signal which could be correlated to vibrations of sulfate group could be observed. Another derivative-like band assigned as δ (CCC) or ν(CC)/δ (CH) is placed in the range of 1029–1050 cm^{-1} in the reference paint spectrum, while the same band is broadened and has its maximum at 1043 cm^{-1} in the spectrum of the aged ARS paint layer. Degradation of ARS colorant after ageing is visible also in the absence of combination band of CC stretching and CCC in-plane-bending vibrations placed at 1022 cm^{-1}. The spectral region below 1000 cm^{-1} shows several derivative and/or inverted signals belonging to ARS molecule vibrations (see Table 3 and Fig. 7). In this region, many characteristic bands of ARS molecule disappear during the ageing process (i.e., δ (C = O)/δ (CCC), γ (C-H)/γ (C-O), γ (C = O)/γ (C-O)/τ (CCCC) and γ (C = O)/γ (C-O)).

The other changes comparing both, aged and non-aged ARS spectra in non-fatty egg tempera are related to proteinaceous binder. Shoulder in the reference spectrum at about 1645 cm^{-1} correlates to fundamental stretching of the amid carbonyl group, while in the aged spectrum this band is overlapped with the medium strong signal of carbonyl-stretching vibrations at 1660 cm^{-1} of ARS molecule. The loss of intensity as well as broadening is present in another characteristic protein band, amid II. Moreover, the reduction of relative intensity is visible also in signals of stretching vibrations of methylene and carbonyl group after ageing (see Table 3).

Also in this case, bassanite in the ground layer was identified in the NIR range (combination band at 5212 cm^{-1}), as a consequence of dehydration of gypsum during ageing.

3.3.2. Transmission FTIR spectroscopy

Fig. 8 illustrates the comparison of two transmission FTIR spectra obtained on the aged and non-aged ARS paint layers in non-fatty egg tempera. The spectral characterization of non-aged ARS paint layers, which contain two strong characteristic absorption bands of C = O stretching vibrations at 1660 cm^{-1} and 1635 cm^{-1} dedicated to ARS molecule, have changed after ageing and appear in the spectrum as one broadened band with maximum at 1635 cm^{-1}. Moreover, this band has a shoulder at ~1657 cm^{-1}, which could be attributed to one of the carbonyl-stretching vibrations of ARS molecule or to amid I from the egg tempera binder (see Fig. 8 and Table 3).

Slight decrease of relative intensity is visible in the signals of proteinaceous binder in the CH stretching region. Carbonyl-stretching vibration of egg tempera binder is broadened after ageing, as well as shifted to lower wave numbers for approximately 25 cm^{-1}. The mentioned downshift of ν(C = O) band may be present due to oxidation of the triglycerides in aged egg yolk [57,58]. Another observable change takes place in the range of bending vibrations of methyl group. This medium strong band placed at 1486 cm^{-1}, corresponds to proteinaceous binder,

Table 3
Numerical frequencies observed in reflection and transmission FTIR spectra of the ARS paint layers in non-fatty egg tempera before and after artificial ageing.

Transmission FTIR[a] (cm^{-1})		Reflection FTIR[a] (cm^{-1})		Band assignment[b]	
Before ageing	After ageing	Before ageing	After ageing	Alizarin red S [28,29,42,43,44,45]	Egg tempera [46]
		583–610	595 vw	skeletal vibrations	
640 m	639 m	645 m	615–650		
678 w	667 w	671–702		γ (C = O)/δ (CCC)	
686 w	689 vw				
712 s	712 m	700–725	715 inverted	γ (C = O)/γ (C-O)	
729 vw	733 vw			δ (CCC)	
766 w		750–770		γ (C-H)/γ (C = O)/τ (CCCC)	
789 w	789 w	791 m	770–800		
824 vw	825 vw	815–835		γ (C-H)/γ (C-O)	
868 w	870 w	871 m			
930 w	930 w	932 m			
1018 s	1018 m	1022 m		ν (CC)/δ (CCC)	
1038 s, 1044 s	1041 s	1029–1050	1043 m, br	δ (CCC) //ν(CC)/δ (CH)	
1069 s	1075 m	1075 m	1090 m, br	υ_S (SO_3)	
1103 m					
1158 vs	1160 vs, br	1135–1200	1142 br, vw	υ_{AS} (SO_3)	
1203 vs	1201 s	1208 m	1210 m	ν (C = O)/δ (CCC)	
1235 vs		1239 s		hydrous SO_3	
1261 vs	1266 s	1269 s		υ (1-C-O)	
1288 s				υ (2-C-O)	
1330 s				ν (CC)	
1348 s	1344 s	1354 s		ν (C-C)/δ (COH)	
1417 m		1415 m	1415 m		
1444 s	1455 sh			ν (CC) arom.	
1463 s	1468 s	1465 s	1463 m	ν (CC)/δ (COH)/δ (CH)	
1486 m					δ (CH_3)
1546 m	1548 m	1549 s	1549 m, br		Amid II
1592 s	1590 s	1591 s		ν (CC) arom.	
1635 vs	1635 m	1645 sh		ν (9-C = O)	Amid I
1660 s	1657 sh	1661 vs	1660 m, br	ν (10-C = O)	
1740 s	1724 m, br	1741 vs	1737 s		ν (C = O)
2855 s	2855 m	2858 vs	2858 s		ν_S (CH_2)
2926 vs	2924 m	2929 vs	2929 s		ν_{AS} (CH_2)
3070 w, sh	3070 vw	3080 m	3080 m	intramolecular hydrogen bonding ν (OH)	
3278 s, br	3265 w, br	3290 vs	3290 vs		ν (NH)
3451 s, br	3441 w, br			ν (OH)	

[a] vw—very weak, w—weak, m—medium, s—strong, vs—very strong, sh—shoulder, br—broad.
[b] ν—stretching, δ—in-plane bending, γ—out-of-plane bending, τ—torsion.

and disappears after ageing. Furthermore, a reduction in intensities, likewise broadening, of two characteristic signals in OH/NH stretching region placed at 3441 and 3265 cm^{-1}, respectively, were observed.

Peaks attributed to aromatic CC stretching vibrations at 1592 cm^{-1} and combination of ν(CC)/δ(COH)/δ(CH) vibrations at 1463 cm^{-1} remained almost unchanged after ageing, whereas additional signal of the aforementioned vibration at 1444 cm^{-1} is shifted for ~10 cm^{-1}

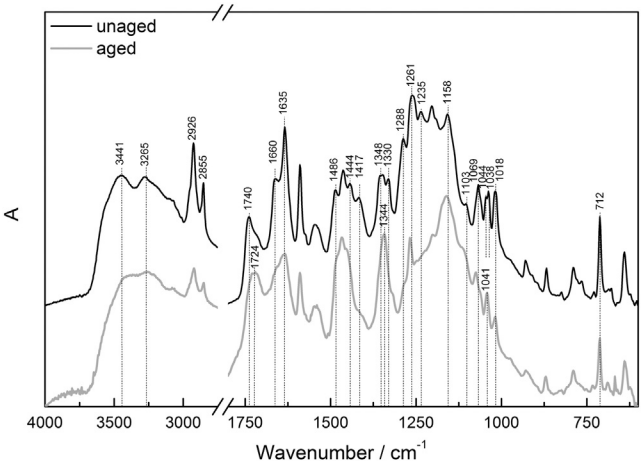

Fig. 8. Transmission FTIR spectra of unaged (black spectrum) and aged (gray spectrum) ARS egg tempera paint layers. Spectra are translated upon vertical axis for ease of comparison. The most representative differences between spectra are labelled.

and is present as shoulder of stronger ν(CC)/δ(COH)/δ(CH) band. Moreover, medium strong signal of unassigned vibration placed at 1417 cm^{-1} is no longer visible after ageing. Distinctive strong doublet at 1348 and 1330 cm^{-1}, assigned to combination of ν(C-C)/δ(COH) and CC stretching vibration, respectively, is present as single band after ageing with maximum at 1344 cm^{-1}. The C-O stretching region shows shifting and intensity reduction of the band placed at 1261 cm^{-1} and the disappearance of the signal placed at 1288 cm^{-1}.

The transmission spectrum obtained on the aged ARS painting layers shows another abandon of hydrous sulfonate stretching vibration band, as well as shifting and intensity decreasing of symmetric stretching vibration of sulfonate group at 1069 cm^{-1}. In comparison to ARS paint layers in lipid binder, the changes in the spectral features of sulfonate regions are not so pronounced.

Another unassigned medium strong band placed at 1103 cm^{-1} after ageing disappears. Double band of δ (CCC) //ν(CC)/δ (CH) in the ARS anthracene skeleton is visible as strong single band after ageing with maximum at 1041 cm^{-1}. Moreover, a reduction of intensity is seen in the absorption bands of ν (CC)/δ (CCC) at 1018 cm^{-1} along with the combination signals of out-of-plane bending of C-O and C = O group at 712 cm^{-1}.

3.3.3. Surface-enhanced Raman spectroscopy (SERS)

Comparing the SERS spectra of ARS powder, aged and unaged spectra of ARS paint layers (Fig. 9), there is a change in spectral pattern based on the inversion of relative intensities of 1427/1443 cm^{-1} doublet. In the spectrum of the unaged paint layer, a shoulder at the 1427 cm^{-1} could be observed, while in the spectrum of aged paint layer relative

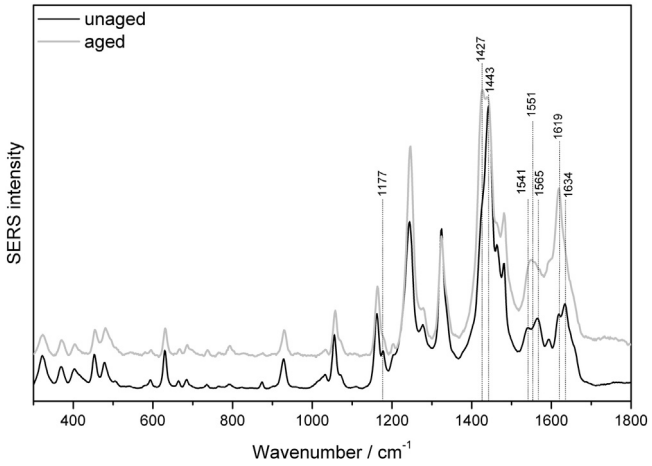

Fig. 9. SERS spectra of unaged (black spectrum) and aged (gray spectrum) ARS egg tempera paint layers. Spectra are translated upon vertical axis for ease of comparison. ($\lambda_0 = 514$ nm, 0.6 mW, 5 s exposure time).

intensity of the band at 1427 cm^{-1} increases. Other changes in the spectrum of aged layers are the weakening of the band at 1177 cm^{-1}, the disappearance of the bands at 1565 and 1541 cm^{-1}, which results in the appearance of a new, broad band at 1551 cm^{-1}. Moreover, the strongest band of the carbonyl-stretching region in the spectrum of unaged paint layer appears at 1634 cm^{-1}, while in the spectrum of aged paint layer a band at 1619 cm^{-1} becomes the strongest in this region. All the changes are associated with different adsorption forms of ARS on silver nanoparticle surface, suggesting the higher contribution of adsorbed ARS in dianionic form in the aged paint layers Similar to results of ARS in linseed oil paint layers, no changes in the spectra related to vibrations of sulfonate group could be observed. The spectral changes could only reflect different adsorption modes of molecule. No significant differences could be observed in comparison to the behaviour of ARS in linseed oil binder.

4. Conclusion

Until this study, not much attention was dedicated to the use of non-invasive reflection spectroscopy for monitoring of degradation processes of organic glaze layers at the surface. As the obtained reflection spectra of aged paint layers could be highly obscured, a careful implementation of supporting methods should be made in order to correctly identify the present material and/or degradation products. Such approach could serve as a platform toward minimally or even non-invasive investigations of the organic glaze layers.

Nevertheless, the deterioration of ARS paint layer (ARS dye in lipid or proteinaceous binder) was for the first time identified by non-invasive reflection FTIR spectroscopy, based on characteristic changes in the spectral regions belonging to carbonyl, hydroxyl, and sulfonate group, as well as anthracene aromatic skeletal vibrational modes. All these spectral differences were confirmed also by the transmission FTIR spectroscopy, although the changes in spectral features were visible to a lesser extent by this method, probably due to sampling as a lower concentration of degraded products are present in the bulk comparing to the surface. Spectral patterns of ARS in the FTIR spectra of aged paint layers were in many cases indistinguishable; therefore, the exact characterization of the dye in the paint layer could be questionable in an unknown sample. In such cases, the complementation of the research with SERS spectroscopy is suggested. In this study, SERS still offered very good spectra of the dye, thanks to the higher sensitivity of the technique. No significant differences between paint layers in linseed oil and egg tempera in their spectral behaviour were detected, most likely due to the sensitivity and selectivity of the technique for the detection of organic dyes. Variations in relative intensities as well as shifting of the certain bands suggested different adsorption modes of ARS with silver nanoparticles, indicating a higher contribution of ARS in dianionic form in the aged paint layers, which could be further possibly correlated to lower concentrations of the dye in the aged paint layers.

The analysis of paint layers using FTIR spectroscopy indicates that the degradation is binder-dependent. It seems that the degradation of ARS in lipid binder is more pronounced. The surface of paint layers in linseed oil was covered with additional transparent layer after ageing. FTIR analysis showed the presence of Na_2SO_4, which was also confirmed by electron and Raman microscopies. Regarding the fact that the changes in the spectral features of sulfonate regions are not so pronounced in the egg tempera binder, it can be concluded that the formation of sodium sulfate is favoured under impact of UV–Vis radiation and relative humidity in the lipid binder as a result of its photo-oxidative degradation [48]. Indeed, it was already shown that ageing processes has much greater impact on degradation of lipid binders as on proteinaceous ones [59].

Strong degradation was detected also in the other parts of multi-layered model painting. Indeed, the UV–Vis radiation and oscillations of temperature and humidity did not affect only the upper most layer of the model painting, but deterioration was evident also in the specific molecular changes of oil and egg tempera media as well as in the ground layer. The latter was corroborated by the discovery of bassanite (the hemihydrate form of gypsum) by non-invasive reflection spectroscopy in the NIR range.

This work might have possible applications on real painting analysis, facilitating determination of degraded organic glaze layers with non- or minimally invasive techniques.

Acknowledgments

The presented research was supported by the Slovenian Research Agency (grant number L6-4217). This work is also a result of doctoral research, in part financed by the European Union, European Social Fund and the Republic of Slovenia, the Ministry for Education, Science and Sport within the framework of the Operational programme for human resources development for the period 2007–2013 (operation no. 3330-13-500221).

References

[1] J. Kirby, M. Spring, C. Higgitt, The technology of red lake pigment manufacture: study of the dyestuff substrate, Natl. Gall. Tech. Bull. 26 (2005) 71–87.
[2] G. Rath, M. Ndonzao, K. Hostettmann, Antifungal anthraquinones from *Morinda lucida*, Int. J. Pharmacogn. (2015).
[3] J. Wouters, N. Rosario-Chirinos, Dye analysis of pre-Columbian Peruvian textiles with high-performance liquid chromatography and diode-array detection, J. Am. Inst. Conserv. (2013).
[4] B. Szostek, J. Orska-Gawrys, I. Surowiec, M. Trojanowicz, Investigation of natural dyes occurring in historical Coptic textiles by high-performance liquid chromatography with UV–vis and mass spectrometric detection, J. Chromatogr. A 1012 (2003) 179–192.
[5] H. Schweppe, J. Winter, third ed., Artists' Pigments: A Handbook of Their History and Characteristics, vol. 3, National Gallery of Art, Oxford University Press, Oxford, New York, 1997.
[6] E. Gurr, Synthetic Dyes in Biology, Medicine And Chemistry, Academic Press, London, New York, 2012.
[7] A. Holmgren, L. Wu, W. Forsling, Fourier transform infrared and Raman study of alizarin red S adsorbed at the fluorite–water interface, Spectrochim. Acta A Mol. Biomol. Spectrosc. 55 (1999) 1721–1730, http://dx.doi.org/10.1016/S1386-1425(98)00342-4.
[8] H. Puchtler, S.N. Meloan, M.S. Terry, On the history and mechanism of alizarin and alizarin red S stains for calcium, J. Histochem. Cytochem. 17 (1969) 110–124.
[9] L. Jervis, Interaction of immobilised food dye residues with gut proteins, Biochem. Soc. Trans. 24 (1996) 395S.
[10] G. Ackermann, L. Sommer, D. Thorburn Burns, Organic analytical reagents for the determination of inorganic substances, in: R.D. Lide (Ed.), CRC Handb. Chem. Physics, 95th ed.CRC Press/Taylor and Francis, Boca Raton, Florida 2009, p. 2704.
[11] M.K. Cyrański, M.H. Jamróz, A. Rygula, J.C. Dobrowolski, Ł. Dobrzycki, M. Baranska, On two alizarin polymorphs, CrystEngComm 14 (2012) 3667.
[12] K. Gollnick, S. Held, D.O. Mártire, S.E. Braslavsky, Hydroxyanthraquinones as sensitizers of singlet oxygen reactions: quantum yields of triplet formation and singlet

oxygen generation in acetonitrile, J. Photochem. Photobiol. A Chem. 69 (1992) 155–165.
[13] C.J.S. Ibsen, H. Birkedal, Modification of bone-like apatite nanoparticle size and growth kinetics by alizarin red S, Nanoscale 2 (2010) 2478–2486.
[14] E. Svobodová, Z. Bosáková, M. Ohlídalová, M. Novotná, I. Němec, The use of infrared and Raman microspectroscopy for identification of selected red organic dyes in model colour layers of works of art, Vib. Spectrosc. 63 (2012) 380–389, http://dx.doi.org/10.1016/j.vibspec.2012.09.003.
[15] S.A. Centeno, J. Shamir, Surface enhanced Raman scattering (SERS) and FTIR characterization of the sepia melanin pigment used in works of art, J. Mol. Struct. 873 (2008) 149–159, http://dx.doi.org/10.1016/j.molstruc.2007.03.026.
[16] E. Marengo, M.C. Liparota, E. Robotti, M. Bobba, Monitoring of paintings under exposure to UV light by ATR-FT-IR spectroscopy and multivariate control charts, Vib. Spectrosc. 40 (2006) 225–234.
[17] M. Koperska, T. Łojewski, J. Łojewska, Vibrational spectroscopy to study degradation of natural dyes. assessment of oxygen-free cassette for safe exposition of artefacts, Anal. Bioanal. Chem. 399 (2011) 3271–3283.
[18] T. Wu, Guangming Liu, Jincai Zhao, Photoassisted degradation of dye pollutants. 8. Irreversible degradation of alizarin red under visible light radiation in air equilibrated aqueous TiO_2 dispersions, Environ. Sci. Technol. 33 (1999) 2081–2087.
[19] E. Marengo, M.C. Liparota, E. Robotti, M. Bobba, Multivariate calibration applied to the field of cultural heritage: analysis of the pigments on the surface of a painting, Anal. Chim. Acta 553 (2005) 111–122, http://dx.doi.org/10.1016/j.aca.2005.07.061.
[20] T. Del Giacco, L. Latterini, F. Elisei, Photophysical and photochemical properties of 1,2,4-trihydroxy-9,10-anthraquinone adsorbed on inorganic oxides, Photochem. Photobiol. Sci. 2 (2003) 681–687.
[21] M. Hovaneissian, P. Archier, C. Vieillescazes, Influence of cetophenolic and diphenolic intramolecular hydrogen bonding on the chromatographic and spectroscopic properties of hydroxyanthraquinones, Dyes Pigments 74 (2007) 706–712, http://dx.doi.org/10.1016/j.dyepig.2006.05.003.
[22] C. Miliani, F. Rosi, A. Daveri, B.G. Brunetti, Reflection infrared spectroscopy for the non-invasive in situ study of artists' pigments, Appl. Phys. A Mater. Sci. Process. 106 (2012) 295–307, http://dx.doi.org/10.1007/s00339–011-6708-2.
[23] L. Monico, F. Rosi, C. Miliani, A. Daveri, B.G. Brunetti, Non-invasive identification of metal-oxalate complexes on polychrome artwork surfaces by reflection mid-infrared spectroscopy, Spectrochim. Acta A Mol. Biomol. Spectrosc. 116 (2013) 270–280.
[24] W. Vetter, M. Schreiner, Characterization of pigment-binding media systems: comparison of non-invasive in-situ reflection FTIR with transmission FTIR microscopy, E-Preserv. Sci. 8 (2011) 10–22.
[25] M. Leona, J. Stenger, E. Ferloni, Application of surface-enhanced Raman scattering techniques to the ultrasensitive identification of natural dyes in works of art, J. Raman Spectrosc. 37 (2006) 981–992, http://dx.doi.org/10.1002/jrs.1582.
[26] F. Casadio, M. Leona, J.R. Lombardi, R. Van Duyne, Identification of organic colorants in fibers, paints, and glazes by surface enhanced Raman spectroscopy, Acc. Chem. Res. 43 (2010) 782–791, http://dx.doi.org/10.1021/ar100019q.
[27] C.L. Brosseau, K.S. Rayner, F. Casadio, C.M. Grzywacz, R.P. Van Duyne, Surface-enhanced Raman spectroscopy: a direct method to identify colorants in various artist media, Anal. Chem. 81 (2009) 7443–7447, http://dx.doi.org/10.1021/ac901219m.
[28] M.V. Cañamares, J.V. Garcia-Ramos, C. Domingo, S. Sanchez-Cortes, Surface-enhanced Raman scattering study of the adsorption of the anthraquinone pigment alizarin on Ag nanoparticles, J. Raman Spectrosc. 35 (2004) 921–927, http://dx.doi.org/10.1002/jrs.1228.
[29] M.V. Cañamares, J.V. Garcia-Ramos, C. Domingo, S. Sanchez-Cortes, Surface-enhanced Raman scattering study of the anthraquinone red pigment carminic acid, Vib. Spectrosc. 40 (2006) 161–167, http://dx.doi.org/10.1016/j.vibspec.2005.08.002.
[30] I.T. Shadi, B.Z. Chowdhry, M.J. Snowden, R. Withnall, Semi-quantitative analysis of alizarin and purpurin by surface-enhanced resonance Raman spectroscopy(SERRS) using silver colloids, J. Raman Spectrosc. 35 (2004) 800–807, http://dx.doi.org/10.1002/jrs.1199.
[31] M.L. De Souza, P. Corio, Surface-enhanced Raman scattering study of alizarin red S, Vib. Spectrosc. 54 (2010) 137–141, http://dx.doi.org/10.1016/j.vibspec.2010.07.010.
[32] B. Doherty, B.G. Brunetti, A. Sgamellotti, C. Miliani, A detachable SERS active cellulose film: a minimally invasive approach to the study of painting lakes, J. Raman Spectrosc. 42 (2011) 1932–1938, http://dx.doi.org/10.1002/jrs.2942.
[33] C. Lofrumento, M. Ricci, E. Platania, M. Becucci, E. Castellucci, SERS detection of red organic dyes in Ag-agar gel, J. Raman Spectrosc. 44 (2013) 47–54, http://dx.doi.org/10.1002/jrs.4162.
[34] F. Pozzi, J.R. Lombardi, S. Bruni, M. Leona, Sample treatment considerations in the analysis of organic colorants by surface-enhanced Raman scattering, Anal. Chem. 84 (2012) 3751–3757, http://dx.doi.org/10.1021/ac300380c.
[35] A. Idone, M. Aceto, E. Diana, L. Appolonia, M. Gulmini, Surface-enhanced Raman scattering for the analysis of red lake pigments in painting layers mounted in cross sections, J. Raman Spectrosc. 45 (2014) 1127–1132, http://dx.doi.org/10.1002/jrs.4491.
[36] A. Campion, P. Kambhampati, Surface-enhanced Raman scattering, Chem. Soc. Rev. 27 (1998) 241–250, http://dx.doi.org/10.1039/a827241z.
[37] W.E. Doering, S.M. Nie, Single-molecule and single-nanoparticle SERS: examining the roles of surface active sites and chemical enhancement, J. Phys. Chem. B 106 (2002) 311–317, http://dx.doi.org/10.1021/jp011730b.
[38] X.-M. Qian, S.M. Nie, Single-molecule and single-nanoparticle SERS: from fundamental mechanisms to biomedical applications, Chem. Soc. Rev. 37 (2008) 912–920, http://dx.doi.org/10.1039/b708839f.
[39] K. Wehlte, The Materials and Techniques of Painting, Kremer Pigments Incorporated, Aichstetten, New York, 1975.
[40] R. Hudoklin, Tehnologije materialov, ki se uporabljajo v slikarstvu, Vzajemnost, Ljubljana, 1958.
[41] K. Retko, P. Ropret, R. Cerc Korošec, Surface-enhanced Raman spectroscopy (SERS) analysis of organic colourants utilising a new UV-photoreduced substrate, J. Raman Spectrosc. 45 (2014) 1140–1146, http://dx.doi.org/10.1002/jrs.4533.
[42] T. Moriguchi, S. Nakagawa, F. Kaji, Adsorbability of alizarin red S on Fe(III)- and Pb(II)-treated hydroxyapatites in water, Phosphorus Res. Bull. 24 (2010) 62–72, http://dx.doi.org/10.3363/prb.24.62.
[43] P.M. Jayaweera, T.A.U. Jayarathne, Acid/base induced linkage isomerization of alizarin red adsorbed onto nano-porous TiO_2 surfaces, Surf. Sci. 600 (2006)http://dx.doi.org/10.1016/j.susc.2006.08.027.
[44] A. Periasamy, S. Muruganand, M. Palaniswamy, Vibrational studies of Na_2SO_4, K_2SO_4, $NaHSO_4$ and $KHSO_4$ crystals, Rasayan J. Chem. 2 (2009) 981–989.
[45] T. Moriguchi, K. Yano, S. Nakagawa, F. Kaji, Elucidation of adsorption mechanism of bone-staining agent alizarin red S on hydroxyapatite by FT-IR microspectroscopy, J. Colloid Interface Sci. 260 (2003) 19–25, http://dx.doi.org/10.1016/S0021-9797(02)00157-1.
[46] R. Mazzeo, S. Prati, M. Quaranta, E. Joseph, E. Kendix, M. Galeotti, Attenuated total reflection micro FTIR characterisation of pigment-binder interaction in reconstructed paint films, Anal. Bioanal. Chem. 392 (2008) 65–76, http://dx.doi.org/10.1007/s00216-008-2126-5.
[47] L. Brambilla, C. Riedo, C. Baraldi, A. Nevin, M.C. Gamberini, C. D'Andrea, et al., Characterization of fresh and aged natural ingredients used in historical ointments by molecular spectroscopic techniques: IR, Raman and fluorescence, Anal. Bioanal. Chem. 401 (2011) 1827–1837, http://dx.doi.org/10.1007/s00216-011-5168-z.
[48] M. Lazzari, O. Chiantore, Drying and oxidative degradation of linseed oil, Polym. Degrad. Stab. 65 (1999) 303–313, http://dx.doi.org/10.1016/S0141-3910(99)00020-8.
[49] J. Mallégol, J.-L. Gardette, J. Lemaire, Long-term behavior of oil-based varnishes and paints. Photo- and thermooxidation of cured linseed oil, J. Am. Oil Chem. Soc. 77 (2000) 257–263, http://dx.doi.org/10.1007/s11746–000-0042-4.
[50] M. Vagnini, C. Miliani, L. Cartechini, P. Rocchi, B.G. Brunetti, A. Sgamellotti, FT-NIR spectroscopy for non-invasive identification of natural polymers and resins in easel paintings, Anal. Bioanal. Chem. 395 (2009) 2107–2118, http://dx.doi.org/10.1007/s00216-009-3145-6.
[51] J. Workman Jr., L. Weyer, Practical Guide to Interpretive Near-Infrared Spectroscopy, CRC Press, Taylor & Francis Group, Boca Raton, London, New York, 2007.
[52] F. Rosi, A. Daveri, B. Doherty, S. Nazzareni, B.G. Brunetti, A. Sgamellotti, et al., On the use of overtone and combination bands for the analysis of the $CaSO_4$–$H2_O$ system by mid-infrared reflection spectroscopy, Appl. Spectrosc. 64 (2010) 956–963, http://dx.doi.org/10.1366/000370210792080975.
[53] K. Ben Mabrouk, T.H. Kauffmann, H. Aroui, M.D. Fontana, Raman study of cation effect on sulfate vibration modes in solid state and in aqueous solutions, J. Raman Spectrosc. 44 (2013) 1603–1608, http://dx.doi.org/10.1002/jrs.4374.
[54] D. Erhardt, C.S. Tumosa, M.F. Mecklenburg, Natural and accelerated thermal aging of oil paint films, Tradit. Innov. Adv. Conserv. Contrib. to IIC Melb. Congr. 10–14 Oct. 2000 2000, pp. 65–69.
[55] J. Mallégol, J.-L. Gardette, J. Lemaire, Long-term behavior of oil-based varnishes and paints I. Spectroscopic analysis of curing drying oils, J. Am. Oil Chem. Soc. 76 (1999) 967–976, http://dx.doi.org/10.1007/s11746–999-0114-3.
[56] H. Lachheb, E. Puzenat, A. Houas, M. Ksibi, E. Elaloui, C. Guillard, et al., Photocatalytic degradation of various types of dyes (alizarin S, crocein Orange G, methyl red, Congo red, methylene blue) in water by UV-irradiated titania, Appl. Catal. B Environ. 39 (2002) 75–90, http://dx.doi.org/10.1016/S0926-3373(02)00078-4.
[57] R.J. Meilunas, J.G. Bentsen, A. Steinberg, Analysis of aged paint binders by FTIR spectroscopy, Stud. Conserv. 35 (1990) 33–51.
[58] V. Dorge, F.C. Howlett (Eds.), Painted Wood: History and Conservation, Getty Conservation Institute, Los Angeles, 1998.
[59] M.P. Colombini, F. Modugno, E. Menicagli, R. Fuoco, A. Giacomelli, GC–MS characterization of proteinaceous and lipid binders in UV aged polychrome artifacts, Microchem. J. 67 (2000) 291–300, http://dx.doi.org/10.1016/S0026-265X(00)00075-8.